

Development of a high-resolution fast gamma-ray imager for the new-generation PET II

Kaname INOUE
Hideki KOTAKA
Haruyuki KURODA
Ikuo MORITANI
Yukari YAMAWAKI
Souichiro AOGAKI¹⁾
Fujio TAKEUTCHI

Faculty of Science, Kyoto Sangyo University, Kyoto 603-8555 Japan

1) Faculty of Engineering, Kyoto Sangyo University, Kyoto 603-8555 Japan

Abstract

A lot of effort has been spent again this year for the development of the new readout system of scintillator crystals using wave-length shifter. The main part of the progress we accomplished is reported here.

Introduction

The Positron-Emission Tomography (PET) device based on the current technique is expensive, and this factor, although the device is known to be useful, prohibits the device from becoming popular. We believe that if the read-out method using wave-length shifter (WLS) is successfully applied to the detection of 511 keV gamma rays, PET should be produced with a much lower cost. We have been trying a read-out method using WLS so that many more scintillator crystals are read-out with fewer photomultipliers[1]. This allows to use smaller crystals in size and thus, increases the spatial resolution of detection. We aim at improving it to about 1 mm.

In this study, our main concerns are as follows:

1. How to transport maximum amount of light emitted in the scintillator crystal to the photomultiplier (PM) . We try to understand systematically how the photons are lost at each stage in order to improve the light transmission.
2. How to improve the spatial resolution of the detector. We try to reproduce in a coinci-

dence measurement the good spatial resolution observed in a measurement with one detector with a collimator.

3. We try to estimate the increase of the background effects coming from the Compton scattering and try to find the method to reduce them.

1. and 3. are rather specific to the read-out system we are using. The use of the WLS limits the amount of light, and thus limits the pulse-height resolution. Special care must be taken to avoid background noise coming from the Compton scattering effects which are more difficult to eliminate than in the traditional method.

Last year, by using LuYAP crystals and Kuraray B-2 (800) wave-length shifter, we obtained a spatial resolution of the order of 1 mm (FWHM) for 622 keV gammas from ^{137}Cs . But the amount of light we could obtain was still very low, only 3.5 photoelectrons or so. Last year's study showed that the main loss of photons occurs at the connection between the crystal and the wave-length shifter. This fact was found in the simulation, and was confirmed in an experimental study. We try to find better ways to connect crystals to WLS.

Read-out method using WLS

The photons created in the crystal by the interaction, either the photoabsorption, or Compton scattering with the incoming 511-keV gamma ray have to be transported to the PM by means of a light guide. The light path, however, is bent by 90 degrees, and with an ordinary light guide, this cannot be achieved. In our study, the wave-length shifter (WLS) is used for that purpose.

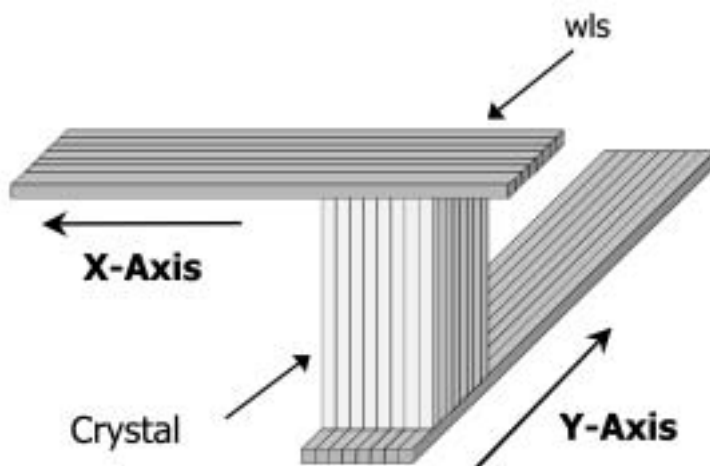


Fig. 1 Read-out method of the crystals using wave-length shifter

The photons hitting the agent in WLS excite it, and in the deexcitation process, a part of the

produced photons emitted isotropically is transported to the PM. One WLS fiber is used to read-out many crystals aligned so as to reduce the cost of construction. Fig. 1 shows how the x- and y-coordinates of the crystals are read-out by WLS.

1. Major modifications in the detection system

1.1 Scintillator crystal used

Our method of using wave-length shifter as a light guide requires the use of emitted wave length of the light to be in the near ultraviolet region, since the quantum efficiency of the bialkali photocathode is maximum at about 410 nm. However, it was shown that LYSO crystal has a larger light yield in terms of photons/MeV than LuYAP crystal we used last year. As we are very much concerned about the amount of light yield, we have decided to try this crystal sacrificing the matching of the wave length of the output of wave-length shifter and the photocathode.

The characteristics of the LYSO crystals we obtained this year are shown in Table 1 in comparison with those of the LuYAP crystal we used last year.

crystal	LuYAP(Ce)	LYSO(Ce)
composition	$\text{Lu}_{0.5}\text{Y}_{0.5}\text{Al O}_3$	$\text{Lu}_{1.8}\text{Y}_{0.2}\text{Si O}_5$
refractive index	1.95	1.82
density g/cm ³	6.5	7.1
effective Z	65	66.4
decay time ns	18	40
yield photons/MeV	9600	27000
wave length nm	370	440

Table 1 Physical properties of the tested scintillator crystals

Note should be taken that the amount of emitted light is 3 times larger, but the decay time is slightly longer.

1.2 Wave-length shifter (WLS)

For the LYSO crystal, we used Y-11 WLS produced by Kuraray. The absorption and emission wave lengths of this WLS are peaked at about 430 nm and 470 nm, respectively as shown in Fig. 2.

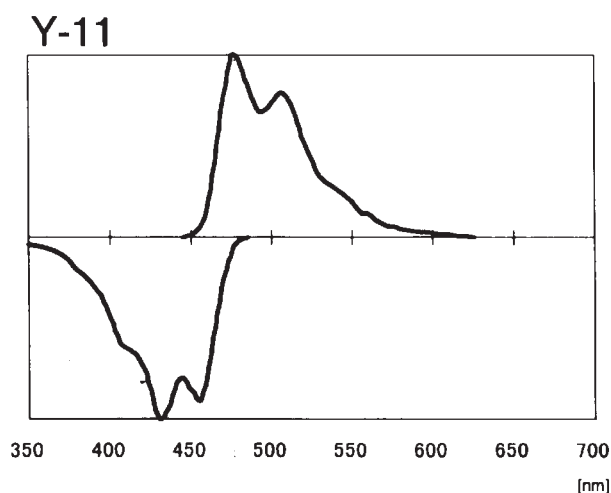


Fig. 2 Absorption and Emission wave-length spectra of Y11 WLS (From Kuraray catalog)

The sensitivity of the bialkali photocathode as a function of the wave length is shown in Fig.

3. There is certainly a mismatch, but the large light yield of LYSO might compensate it. We dis-

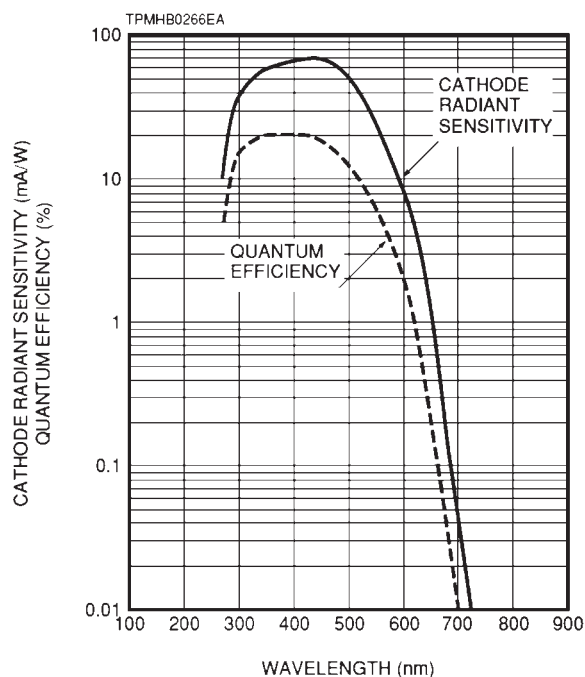


Fig. 3 Bialkali Photocathode sensitivity as a function of the wave length (from Hamamatsu catalog)

cuss the absolute light yield in Chap. 3.

We have experimentally found that the double cladding WLS transmits larger amount of light by about 30% than the single cladding WLS. This is also confirmed by the simulation study presented in Chap. 4. However, the double-clad WLS is available only with a round section. Thus we have chosen Kuraray Y-11 double-clad WLS with a round section of 1mm ϕ .

1.3 Lutetium natural radioactivity

It became clear that the background due to the radioactive ^{176}Lu isotope which is only 2.59% component in the natural lutetium is noticeable. This isotope decays with a lifetime of 3.78×10^{10} years to ^{176}Hf . As shown in the decay scheme in Fig. 4, this isotope emits several gamma rays which can be potentially harmful to us.

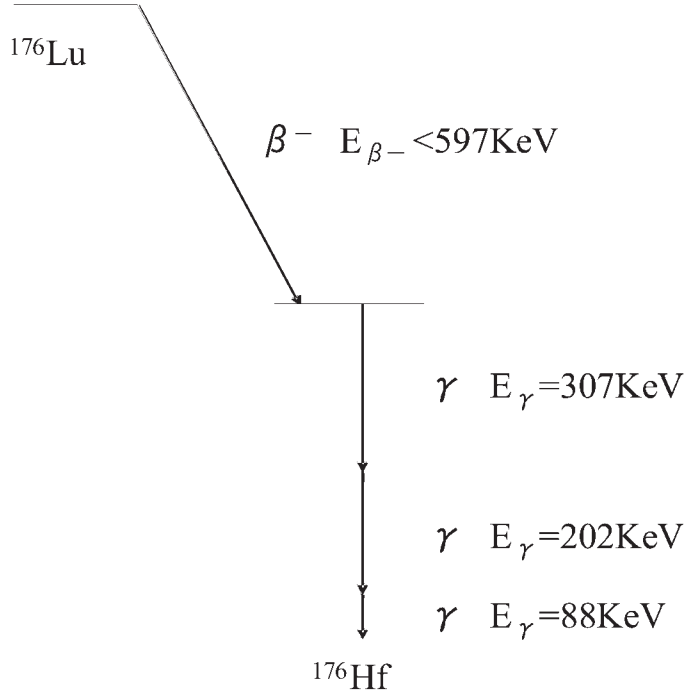


Fig. 4 Decay scheme of ^{176}Lu naturally included in Lu

Last year, we used LuYAP crystal which also contains lutetium, but the effects were not equally noticeable. In a coincidence measurement, this natural radioactivity should not have such an important effect, although it might increase the background. In the past, we measured the spatial resolution with a single pad of crystals and with ^{137}Cs source. This became impossible. Thus this time, to measure the spatial resolution with a single detector, we used $^{22}\text{Na} \beta^+$ source and

measured gamma-rays in coincidence with a NaI(Tl) crystal put on the opposite side which has a larger angular acceptance, as shown in Fig. 5

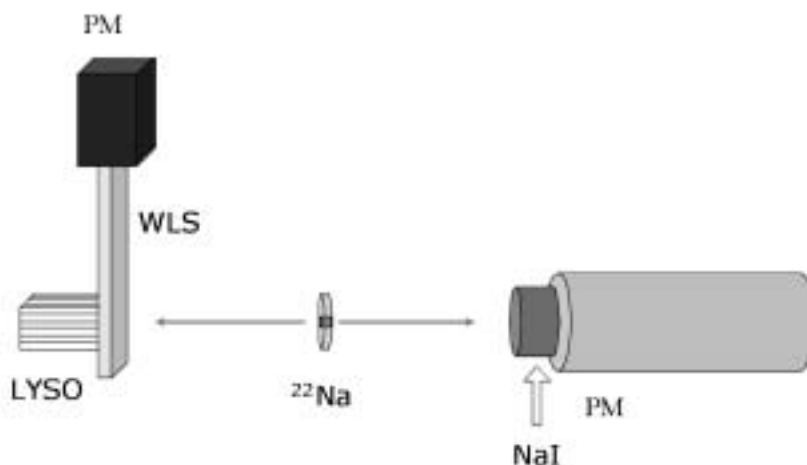


Fig. 5 NaI counter was used in coincidence to remove the effect of the natural lutetium radioactivity.

1.4 Self absorption

The self-absorption effect of the emitted light in the LYSO crystal has not been known. This is, however, a very important number in order to evaluate the amount of light transmitted to the photomultiplier. Also if the self absorption is very large, there is no point in using long crystals.

The measurement was not easy since it is difficult to obtain a long single crystal. We used a 1 mm × 1 mm × 40 mm LYSO crystal and measured the self absorption using the setup shown in Fig. 6.

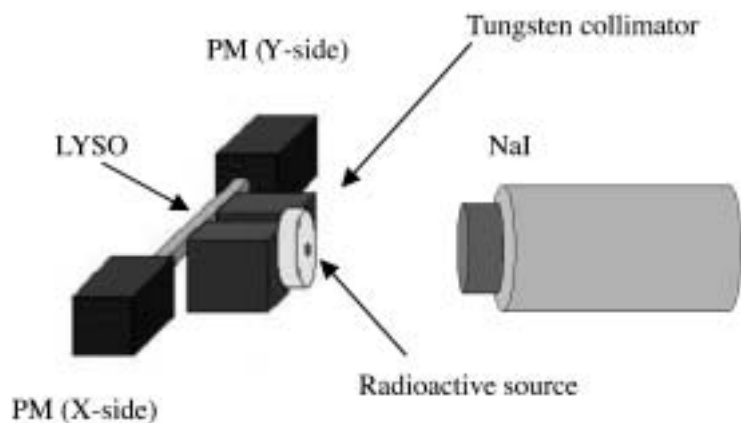


Fig. 6 Setup used to measure the self absorption in the LYSO crystal using tungsten collimator

By fitting the photo-absorption peak of the 511 keV gamma rays in the obtained pulse-height spectra, we tried to find the position of the peak at 3 different positions of the crystal where the collimator was set at a time.

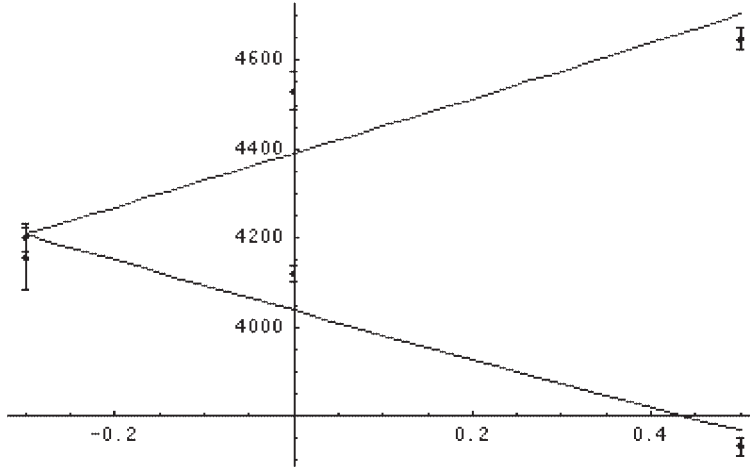


Fig. 7 Photoabsorption peak position was measured at 3 different points of collimator setting. Data are fitted with two exponential curves with a fixed decay length.

The result is shown in Fig. 7. By fitting the data points, we deduced that the self-absorption of the emitted light in the LYSO crystal to be 12.9%/cm.

2. Back Photomultiplier (BPM)

With our method of reading out the light using the WLS, it is not possible to expect a very good pulse-height resolution. As the amount of photoelectrons in the PM is small, it is even difficult to separate the photopeak from the Compton peak. We can, however make use of the detection of 511 keV gamma rays equally well with the photopeak or with the Compton effect. But if a single 511 keV gamma ray enters a crystal, and back-scattered, then enters a very far crystal, where it is absorbed either with a photoelectric or Compton effect, this can cause a large error in reconstructing the source position, if we consider those hit positions to be hit by a pair of gammas emitted back-to-back. To avoid this phenomenon (we call it “backscattering background” in this report), we have to reject coincident detection of a gamma ray leaving very small pulse heights in two crystals far apart.

To obtain the pulse-height information from a pad of crystals, we have tried to measure the light leaked to the back side of the pad together with a light guide of 16 mm × 16 mm × 20 mm.

The photomultiplier used is Hamamatsu R4124 which has a photocathode diameter of 13 mm. The real setup used is shown in Fig. 8.

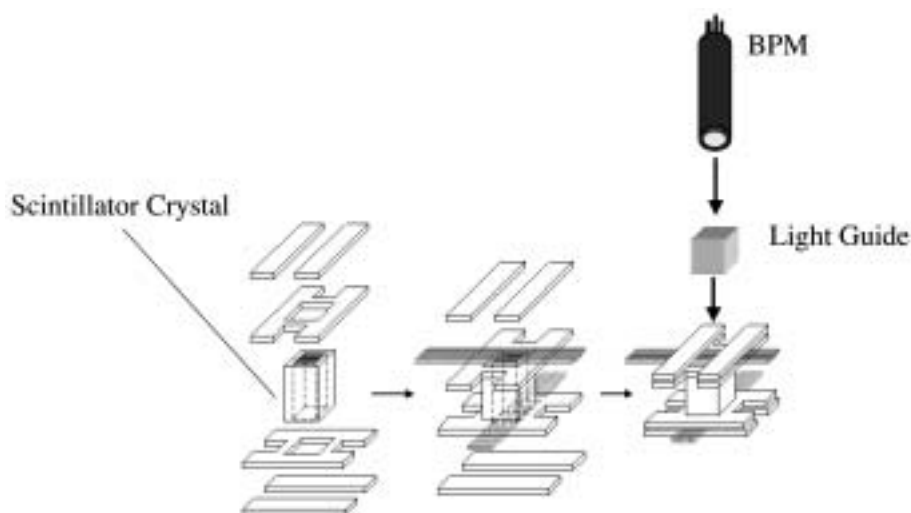


Fig. 8 Figure shows how the WLS is fixed to the scintillator pad. On the back of the WLS layer, the leaked photons are collected with BPM through a light guide.

The typical pulse-height spectrum obtained by using the BPM is shown in Fig. 9.

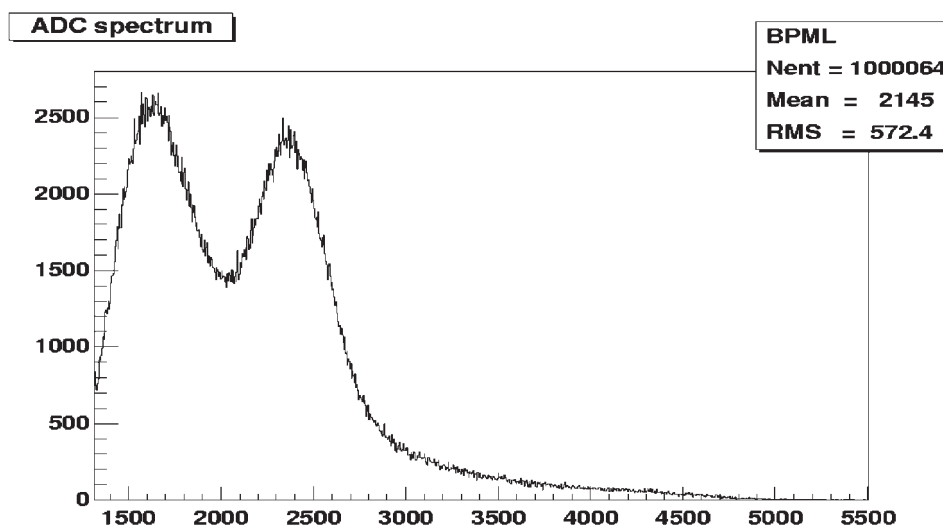


Fig. 9 Pulse-height spectrum obtained with BPM

This spectrum indicates that the light collection is better with BPM than with PM. It might be possible to obtain a better timing information from BPM. We are going to test this point shortly.

3. Crystal-WLS connection

3.1 #9483 film

From the simulation study, it is clear that the largest loss of photons in the transmission from the crystal to the PM is at the connection between the crystal and the WLS. Till now, we did not put any resin nor grease between the crystal and the WLS. With this air gap, the large index of refraction of the crystal repels up to 93% the photons at the end surface of the crystal, according to the simulation.

To fill the gap between the flat end of the crystal and the curved side of the WLS, we tried once in the past, a silicon rubber[2], and found that the insertion of this material clearly improves the light transmission. It was, however, not easy to make a thin layer of silicon rubber, and thus the minimum thickness we could obtain was about 0.3 mm. The light transmission was improved from 3.2 to 4.5 in terms of number of photoelectrons with LuYAP crystal, but the spatial resolution was also slightly deteriorated.

To improve this situation, we tried different materials, and found that 3M highly-transparent film #9483 gave a fairly good result. We have chosen a thickness of 0.125 mm, thus thin enough not to deteriorate the spatial resolution. It is not known how much it is transparent at the wave length of 440 nm, but according to the catalog, it transmits the light of 580 nm up to 90%.

Fig. 10 shows how this film was applied between the crystal and the WLS.

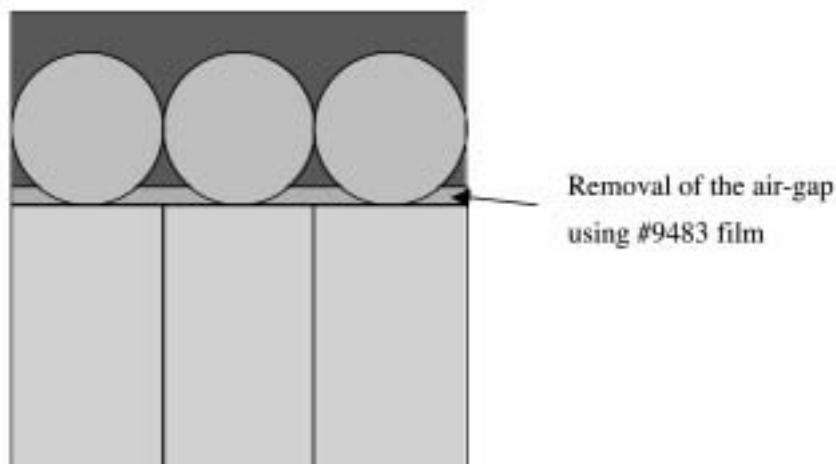


Fig. 10 Using 3M #9483 film, WLS is pressed to the end of crystals. This removes the air gap, and at the same time, round WLS sits with a larger stability.

This time, using LYSO crystal and Y11 WLS, the average number of photoelectrons became 10.2 with #9483 film, and 8.7 without. We conclude that this treatment is very efficient.

3.2 End polishing

This time, the open end of the WLS (the other end goes to the PM) was polished with NIP-PATSU POF cutter, and was wrapped with aluminized mylar as shown in Fig. 11. This again improved the amount of light from 10.2 up to 12.8 photoelectrons.

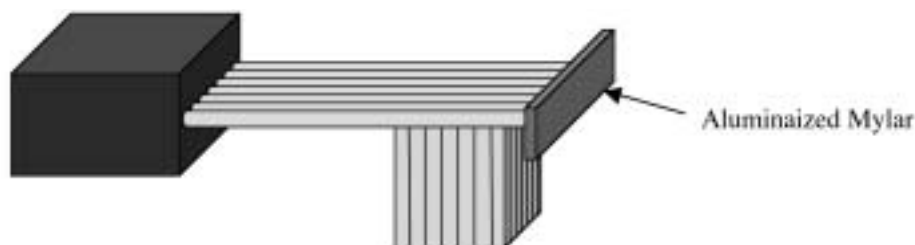


Fig. 11 The open end of the WLS was polished, then an aluminized mylar sheet was applied using optical grease.

The over-all gain with the new crystal and new setup is clear. Fig. 12 shows the pulse-height spectrum thus obtained. The pedestal was at channel 1132, and the single photoelectron peak was observed at channel 1210. From this spectrum, we calculate the transported amount light to PM to be 12.8 photoelectrons.

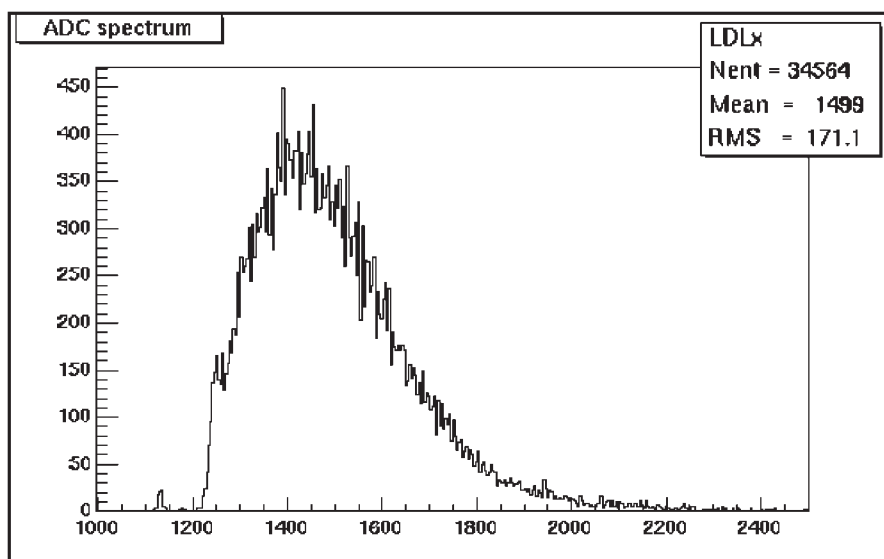


Fig. 12 Using LYSO crystal, Y-11 WLS and 3M #9483 film together with the aluminized endcap, an average pulse height of 12.8 photoelectrons has been obtained.

4. Light transmission study

4.1 Simulation of the light transmission in WLS

Last year, a very extensive study of the photon transmission was carried out using both simulations and experimental tests. This time, we made a simulation of the light transmission in the WLS. What was not very well known was, either or not the total reflection occurs at the interface of the outer clad and the air. If the total reflection occurs there, then the trapping efficiency of the emitted light inside the WLS must be very high.

The responsible of Kuraray Co. said that when the fiber is new, and the surface is very clean, the total reflection actually occurs between the outer clad and the air provided that the length of the WLS is small. To find out the reality, we made a simulation of the trapping efficiency using the geometrical optics and made a comparison with the measurement. We calculated both cases, namely -1) The light is totally absorbed at the surface of the outer clad (like in the case where the fiber is inside a black sheath.) and -2) The interface acts as an agent of the total reflection. We made also a calculation for -a) single-clad fiber, and -b) double-clad fiber. Fig. 13 shows the trapping efficiency in the 4 cases as a function of the light emitting point in the fiber (distance from the central axis.) The trapping efficiency is defined as the part of the light emitted at one point isotropically, transported to one end of the WLS. The absorption of the emitted light in the WLS is negligible for the length of WLS we use. The trapping efficiency increases with the radial distance of the light-emitting point from the central axis.

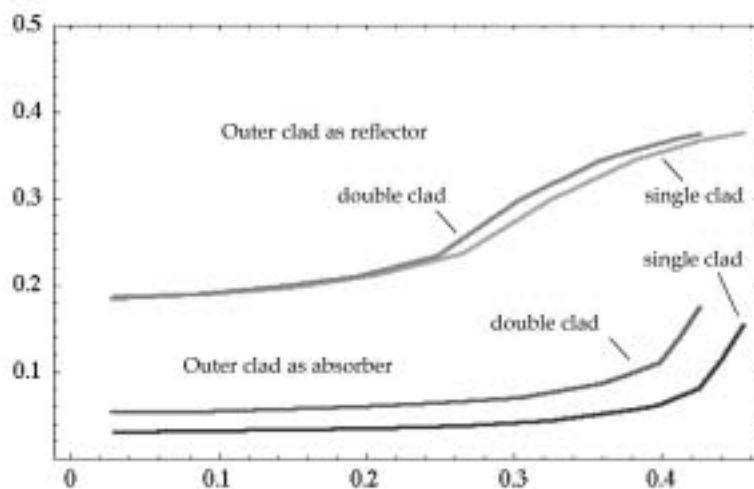


Fig. 13 The trapping efficiency of WLS. The efficiency is plotted as a function of the distance of the light-emitting point from the axis (mm).

The core radius of the 1mm ϕ single-clad fiber is 0.47 mm and the double-clad fiber is 0.44 mm. When the outside of the outer clad is assumed to be a total reflector, naturally the difference between single-clad fiber and the double-clad fiber is small. The trapping ratio Double/Single is 0.998. As the effective core section of the double-clad fiber is smaller, the Double/Single ratio with the core section taken into account is 0.87. For the case where the surface of the outer clad is totally absorptive, Double/Single ratio is 1.44, and even with the difference of the core section taken into account, the ratio is 1.26. Experimentally, we have found that when we use double-clad 1mm ϕ fiber, we have 1.35 times more light than in case four single-clad 0.5 mm \times 0.5 mm square section fiber is used. We have no single-clad 1mm ϕ fiber, and the direct comparison is not possible. But from the above experimental result, it seems that the reality is more close to the case where the outside of the outer clad acts as a total absorber.

4.2 Simulation of the light transmission from the crystal to BPM

It is difficult to estimate the amount of light leak from the back side of the crystal pad to BPM with a simulation. But it is interesting to know this factor to find the conversion efficiency of the light inside the WLS, and also to estimate how much timing resolution we can expect from the BPM signal. The method used was, first we made the pulse-height spectrum at the exit of a single crystal, and then tried to fold a poissonian distribution varying the average until we obtain a spectrum close to the experimentally obtained BPM spectrum.

Fig. 14 shows the pulse-height (or number of photons) per event at the end point of the crystal. In this calculation, the attenuation of 13% per cm was used. The calculation was performed using EGS[3] for LYSO crystal.

As the absorption of 511 keV gamma ray in the crystal is fairly large, the probability of interaction (either photoelectric or Compton) changes quite a bit along the long side of the crystal, as shown in Fig. 15. Thus when the attenuation is present, the pulse-height spectra are different in the two ends as shown in Fig. 14 a) and b).

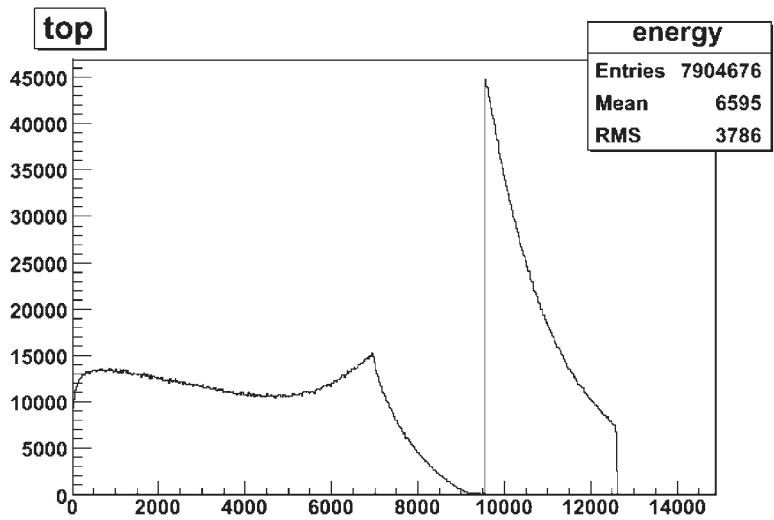


Fig. 14 a)

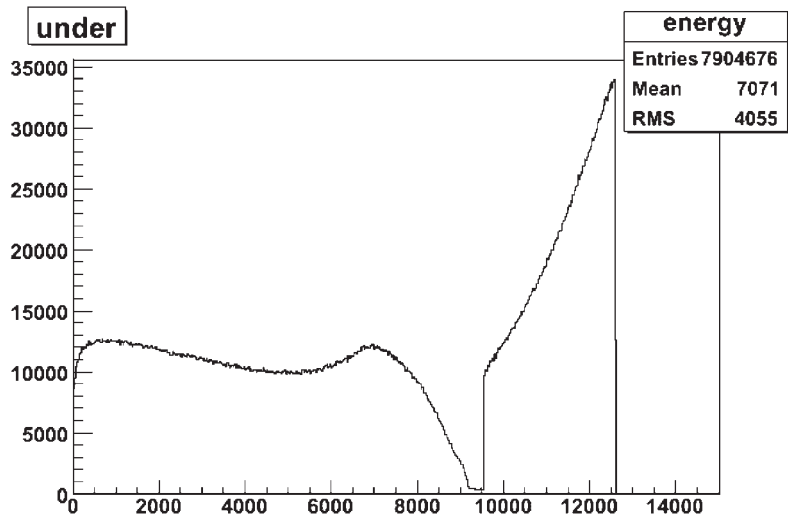


Fig. 14 b) EGS simulation of the light yield at ends of the 20 mm crystal. As the interaction probability is higher near the entrance side of the gamma rays, and the light attenuation is finite, the shapes are different for the rear side of the crystal (top) and the entrance side (bottom).

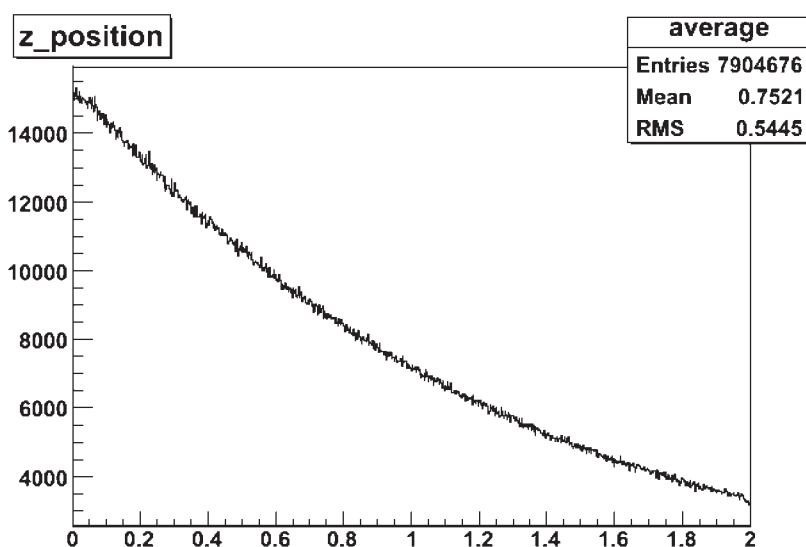


Fig. 15 EGS simulation of the gamma-ray interaction point along the 20 mm crystal. The interaction probability is much higher near the entrance side of the gamma rays to the crystal.

The shape of the folded spectrum was closest to the experimentally obtained BPM spectrum shown in Fig. 16 when the average is 0.007, as shown in Fig. 17.

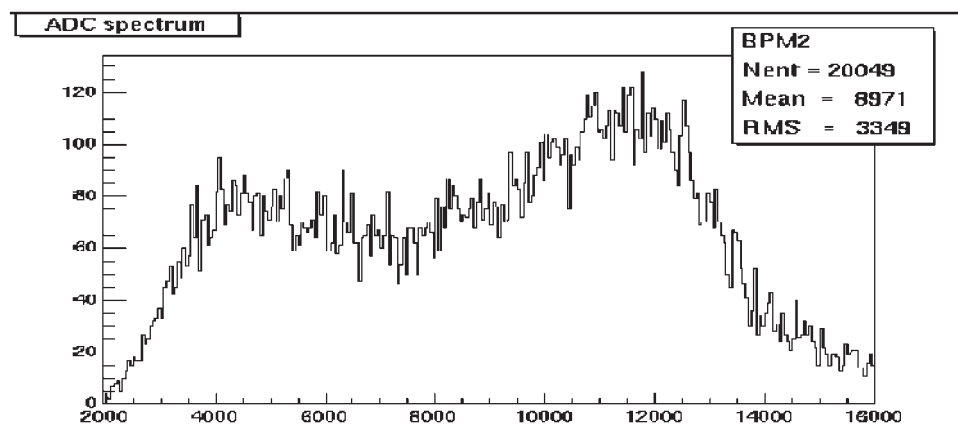


Fig. 16 The observed BPM pulse-height distribution. The BPM is placed on the rear side of the crystal.

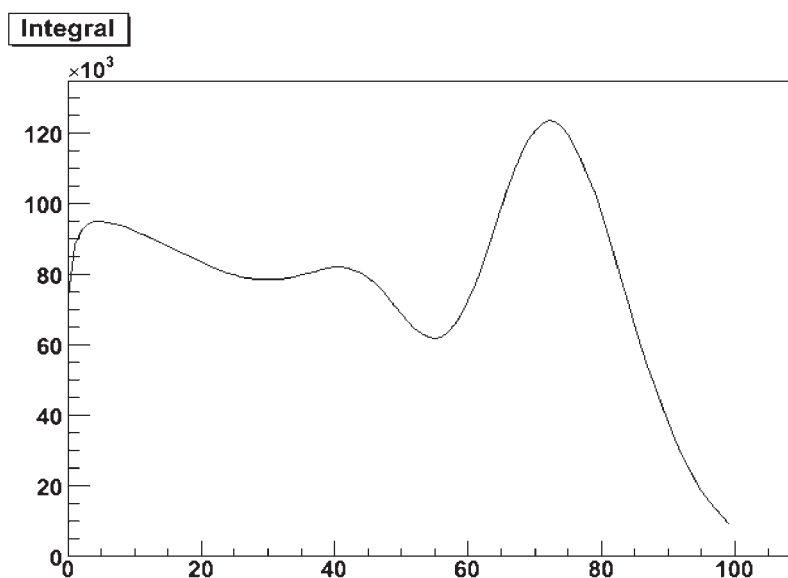


Fig. 17 Spectrum shown in Fig. 14 a) is folded with poissonian distribution with an average of 0.007.

Assuming the probability of extracting photon at the end (7%) and the BPM cathode quantum efficiency (0.2), thus dividing 0.007 by 0.014, we obtain roughly 50 % as the probability of the leakage of the light into the BPM, which looks reasonable.

5. Spatial resolution measurement using a collimator

5.1 Method

In addition to the setup shown in Fig. 5, we have added a collimator made of tungsten with a slit of 0.5 mm. The thickness of the collimator was 4 cm. The collimator was placed just in front of the crystal pad. The slit was oriented parallel to the y-axis. The obtained 2-dimensional histogram is shown in Fig. 18.

By projecting Fig. 18 to the vertical axis, we obtain Fig. 19. By fitting the distribution with a simple Gaussian plus a constant, we obtain 0.44 mm for sigma. The peak height/background ratio was 3.60.

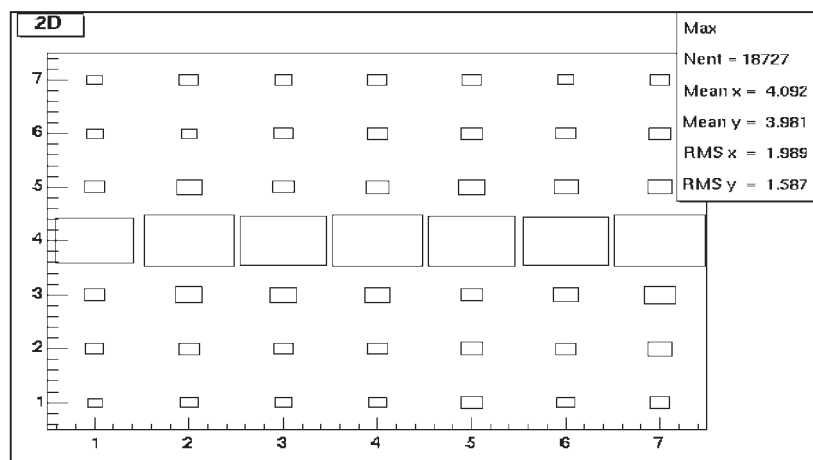


Fig. 18 Two-dimensional histogram obtained with a collimator. The horizontal slit is visible.

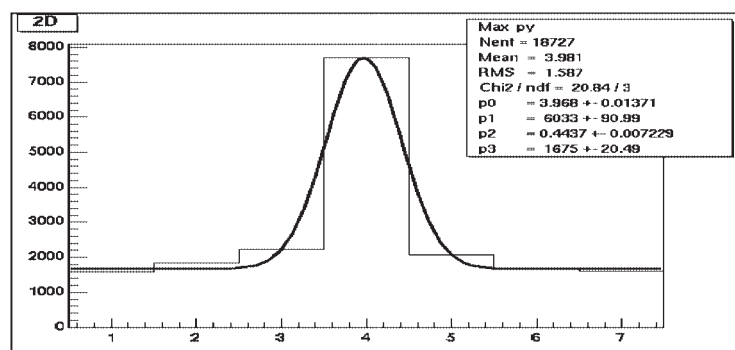


Fig 19 Projection of the two-dimensional histogram to the vertical axis.

5.2 The role of NaI(Tl) counter

We put the NaI counter in coincidence to avoid the effect of natural background due to the Lu radioactivity as explained in Chap. 1.3. It must be also efficient in reducing the effect of 1.83 MeV gamma ray emitted from the ^{22}Na source. Fig. 20 shows the NaI counter spectrum measured in coincidence. The three peaks clearly seen in the spectrum are understood to be, from the right side, the left-over (accidental coincidence) of the 1.83 MeV photopeak, a big 511 keV photopeak, and the Compton scattering peak. By applying a cut on this spectrum to exclude the 1.83 MeV single gamma-rays, (channels 2000 - 7000), we could see that the above-mentioned peak height/background ratio was improved from 3.60 to 7.10.

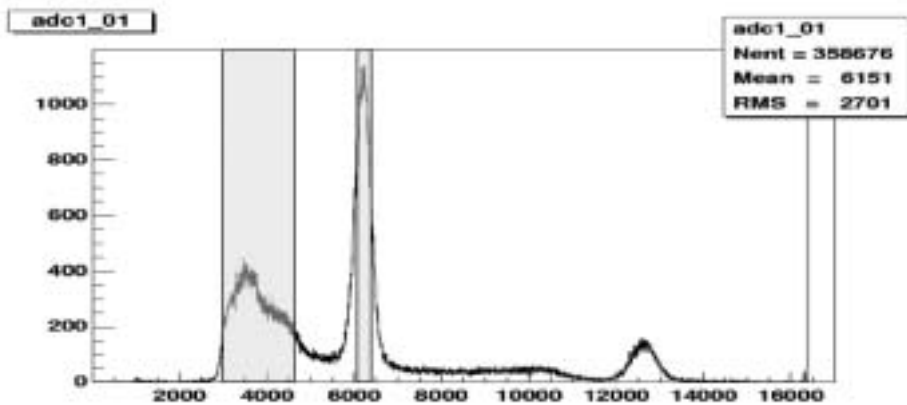


Fig. 20 NaI counter spectrum measured in coincidence. The three peaks clearly seen in the spectrum are understood to be, from the right side, the left-over (accidental coincidence) of the 1.83 MeV photopeak, a big 511 keV photopeak, and the Compton scattering peak.

We are strongly concerned about the backscattering background due to a 500-keV gamma ray Compton-scattered in one crystal in PET and absorbed in a far crystal. To study the effect of one gamma-ray Compton scattered in the NaI crystal in the current setup and detected by the LYSO detector, we tried to apply two separate windows shown in Fig. 20, and compared the corresponding LYSO spectra (Last dynode signal) shown in Fig. 21 a) and b).

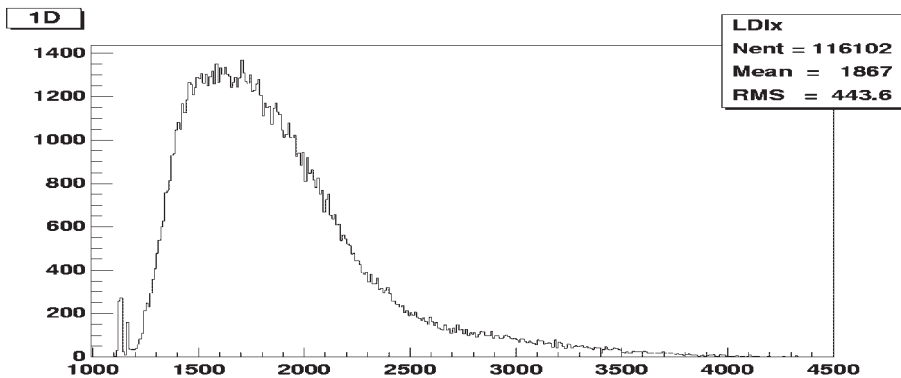


Fig. 21 a) Last dynode spectrum obtained with a gate on NaI spectrum selecting Compton events.

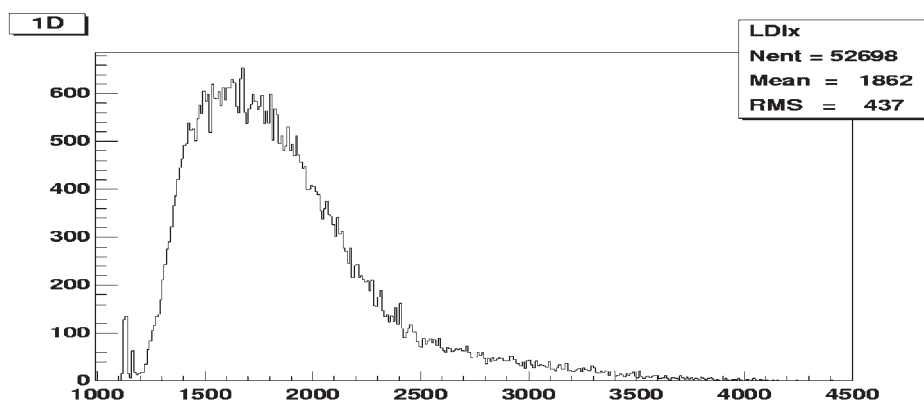


Fig. 21 b) Last dynode spectrum obtained with a gate on NaI spectrum selecting photoabsorption events.

If such a background process is large, the events contained in the Compton peak in Fig. 20 should enhance the low pulse-height region in Fig. 21. In reality, we observe hardly any difference between Fig. 21 a) and b). Therefore, we conclude that the backscattering background is not large here.

5.3 The role of BPM

The BPM spectrum obtained in coincidence is shown in Fig. 22.

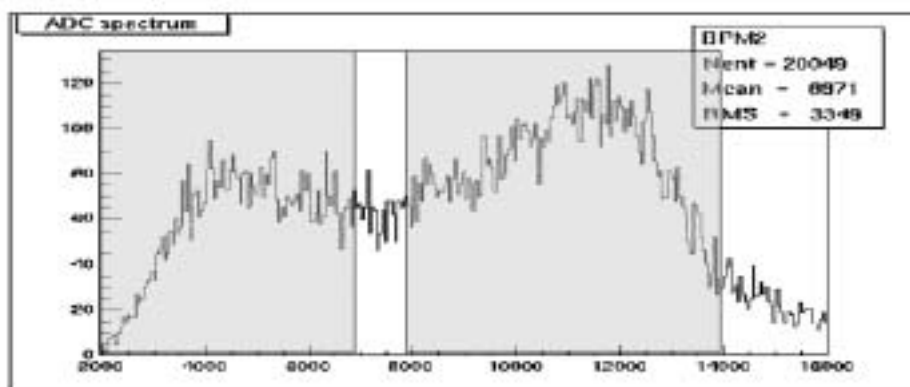


Fig. 22 BPM spectrum obtained in the measurement with a collimator

Two wide peaks are observed, and as we explained in Chap. 4.2, we can understand that the higher peak is mainly the photopeak and the lower peak is due to the Compton process. We try to see the effect of cut on this spectrum. When a window is applied between channel 8000 to 14000, the peak-height/background ratio is improved from 3.60 to 7.10, whereas for the lower window (chan-

nel 2000 - 7000) the ratio was deteriorated to 1.27.

5.4 Time correlation

We applied a cut on the time difference between x and y signal. (width of the window: ~ 3 ns). The peak height/background ratio was improved from 3.60 to 5.82. To reject the accidental coincidence between the NaI and LYSO counter, we also applied a window of a width of ~ 7.5 ns as shown in Fig. 23.

Then the peak-height/background ratio was improved from original 3.60 to 5.93.

By applying all the cuts namely BPM, x-y time difference, and NaI - LYSO time difference, we obtained a peak- height/background ratio of 25.4. Thus by doing so, we should be seeing only the effect of 511 keV gamma ray, which gives a spatial resolution of 0.44 mm (RMS).

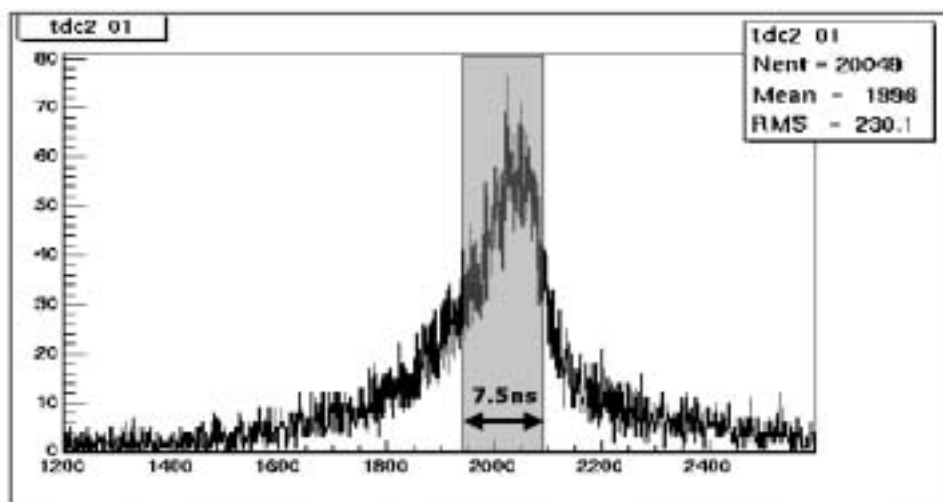


Fig. 23 The time difference spectrum between the last dynode and NaI (resolution 25 ps/chan)

6. Coincidence measurement

6.1 Method

To estimate the spatial resolution of the detector in a more realistic situation, we tried to make a coincidence measurement between two LYSO detectors. The setup is shown schematically in Fig. 24.

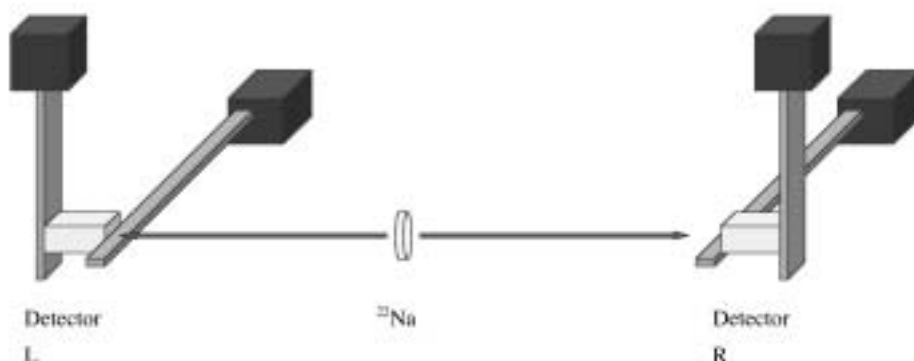


Fig. 24 Setup used in the measurement with two detector in coincidence. Left counter is made of 7×7 crystals, and Right 9×9 crystals.

We made two detectors, making a matrix of 7×7 crystals on the left side, and 9×9 crystals on the right side. The size of each crystal is unchanged, namely $1 \text{ mm} \times 1 \text{ mm} \times 20 \text{ mm}$. We used ^{22}Na β^+ source which was put in the middle.

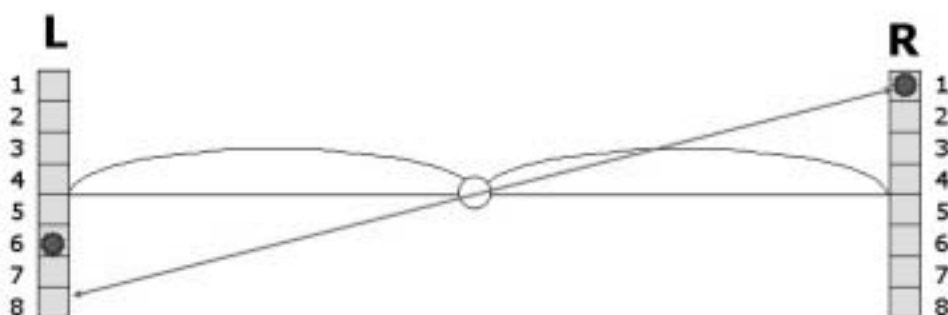


Fig. 25 Definition of the “shift”. See text.

The idea is the following: When crystal 1 is hit on R side, and if the spatial resolution were infinitely good, then we expect to see a hit on the crystal 8 on L side. If in reality, the crystal 6 is hit on L side, we record the “shift” namely the difference 2 between 8 and 6, namely 2 mm.

The spectrum of shift thus obtained is shown in Fig. 26.

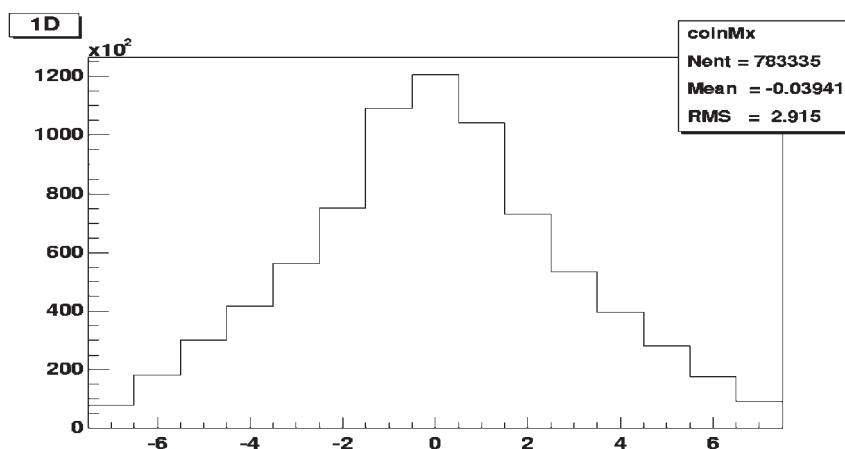


Fig. 26 Histogram of the “shift” obtained in the coincidence measurement (unit: mm)

This spectrum looks like a triangular peak and a narrower peak sitting on top of it. We try to analyze further this spectrum to find out the spatial resolution.

6.2 Effect of backscattering background

We try to estimate the effect of background due to the Compton backscattering by using the BPM spectra obtained in the two detectors. Fig. 27 shows the correlation spectrum between BPM-L and BPM-R.

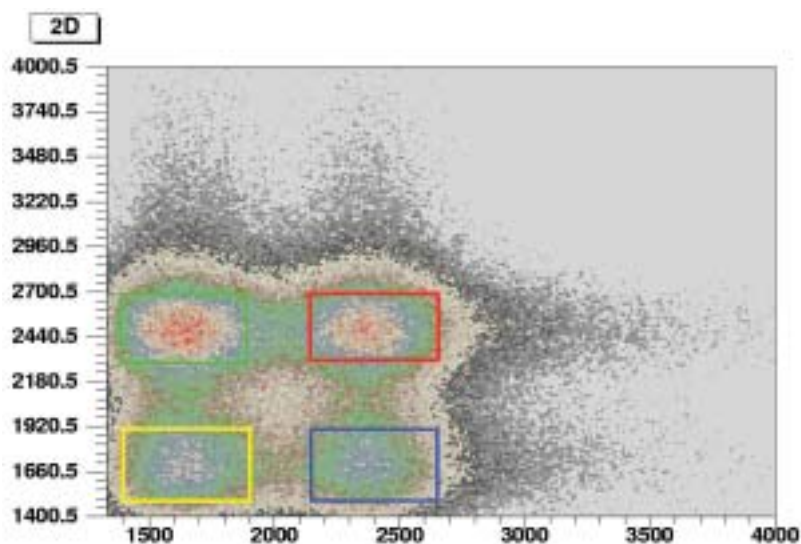


Fig. 27 Correlation between the pulse heights of the BPM's on L (horizontal axis) and R side (vertical axis) Two peaks, corresponding to the photopeak and the Compton peaks, are seen in each counter.

The rectangles shown in Fig. 27 indicates the peaks due to the photoelectric absorption and Compton scattering in both counters. If there were events in which one gamma is Compton-scattered in one of the detectors, then detected again with the opposite detector, the signal should appear in the yellow rectangle as the energy of the scattered gamma is low due to the large scattering angle, about 180 degrees. The ratio of Compton-absorption/photoabsorption of 511 keV gamma ray in a LYSO crystal must be 1.5:1 in the EGS simulation. But in reality, the threshold of the pulse-height is applied at somewhat arbitrary position in each detector, and it is not easy to estimate this ratio in the reality. Thus we try to use the experimental data. This ratio, on L counter is expressed as number of events within blue frame and the red frame which is 1.11:1, whereas for R counter, the number of events within green frame and the red frame which is 0.74:1. Thus the Compton - Compton probability with respect to photoelectric - photoelectric probability from the two real 511 keV gamma rays in coincidence is $1.11 \times 0.74 = 0.82$. In reality the number of events included in the yellow frame is 0.84 times the number of events in the red frame. This means there is almost no space left for the direct Compton - Compton phenomenon originating from one 511 keV gamma ray which can cause backscattering background.

6.3 Timing cuts

The time-difference spectra between L and R counter, x-y on L counter, x-y on R counter are shown in Figs. 28, 29, and 30 respectively.

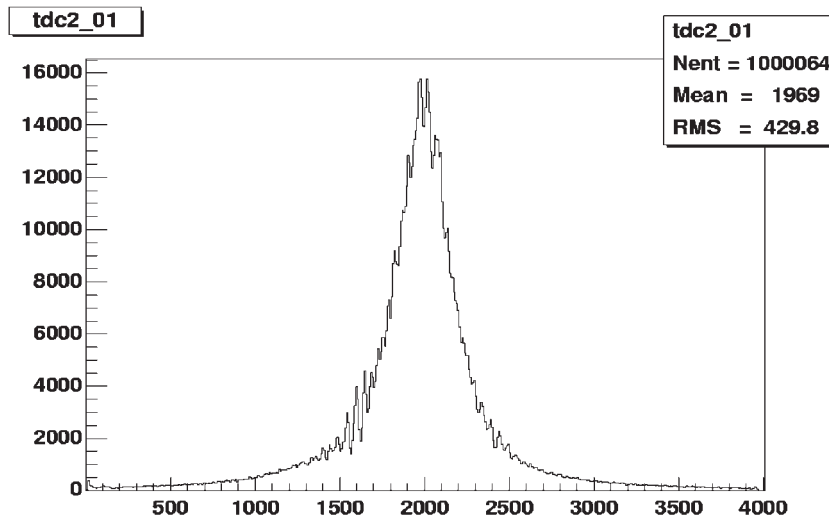


Fig. 28 The time difference spectrum between L and R counter (resolution 25 ps/chan)

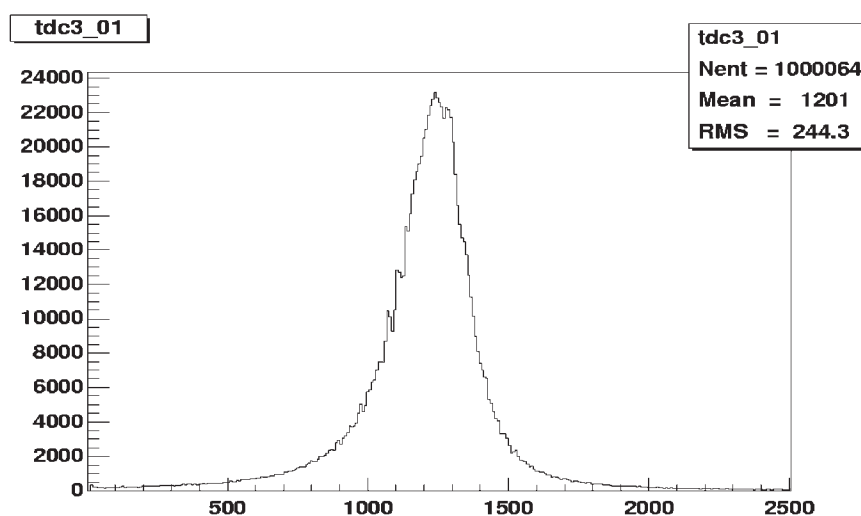


Fig. 29 The time difference spectrum between two last dynodes on L counter(resolution 25 ps/chan)

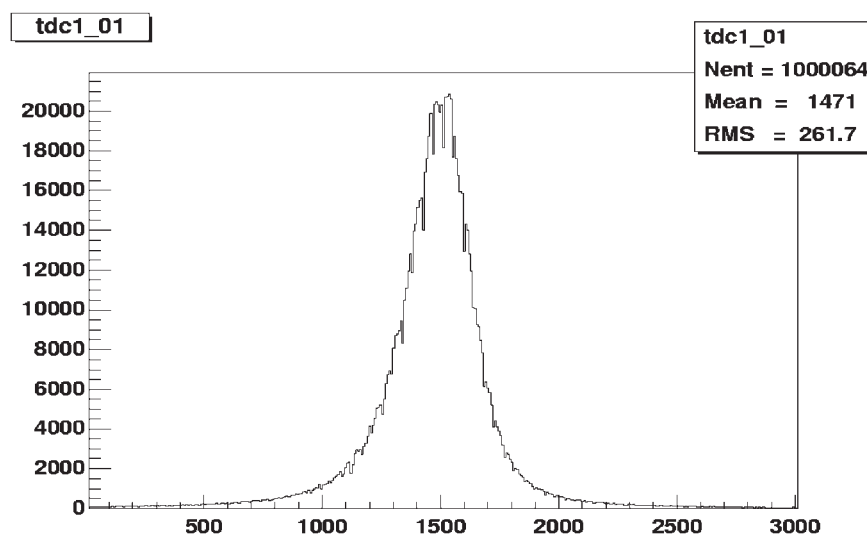


Fig. 30 The time difference spectrum between two last dynodes on R counter(resolution 25 ps/chan)

On all of these timing spectra, a window of ± 4.9 ns was applied.

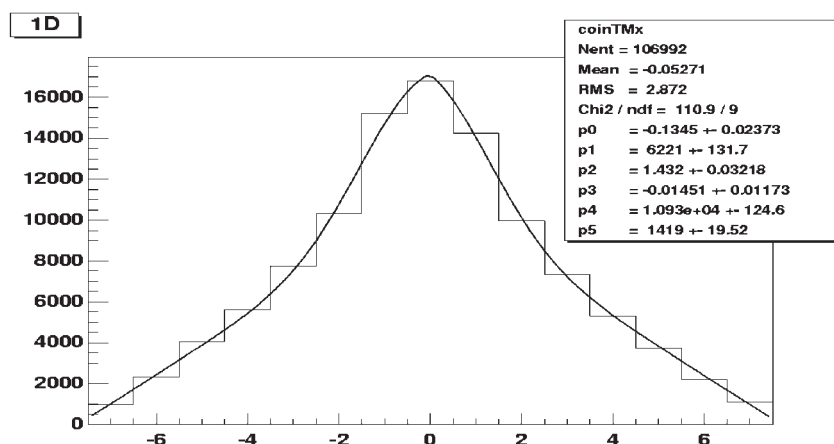


Fig. 31 Shift histogram with windows on the time difference spectra

The result shown in Fig. 31 is slightly improved compared with Fig. 26, but not very much.

6.4 BPM cut

Then we try to see just the photopeak events in both counters. Fig. 32 a) and b) show the BPM counter spectra obtained in each L and R counter, respectively.

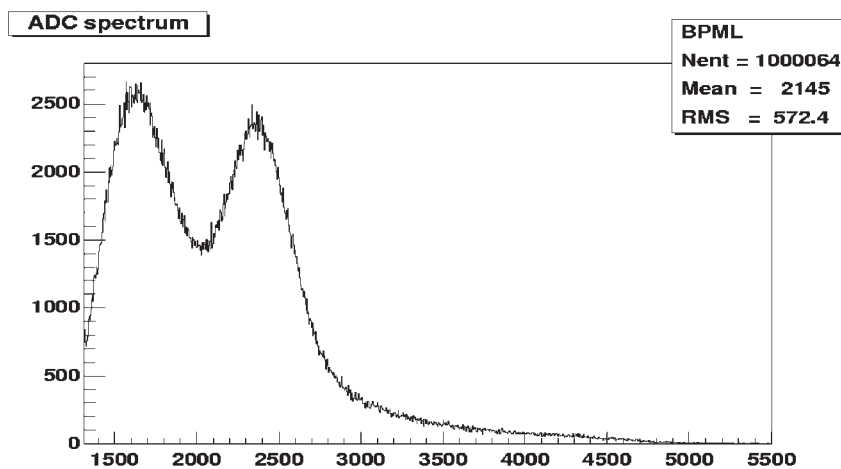


Fig. 32 a) BPM pulse-height spectrum on L counter

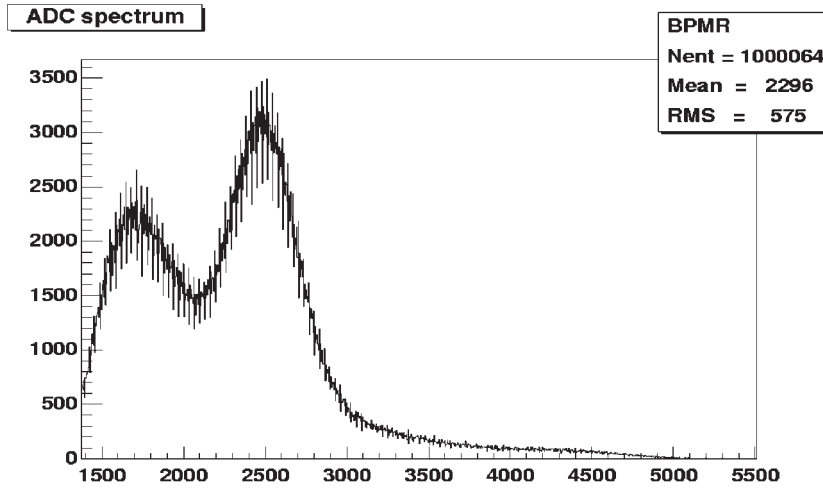


Fig. 32 b) BPM pulse-height spectrum on R counter

We apply a window on L counter channel 2250 - 2450, and R counter 2380 - 2580 respectively. The result is shown in Fig. 33.

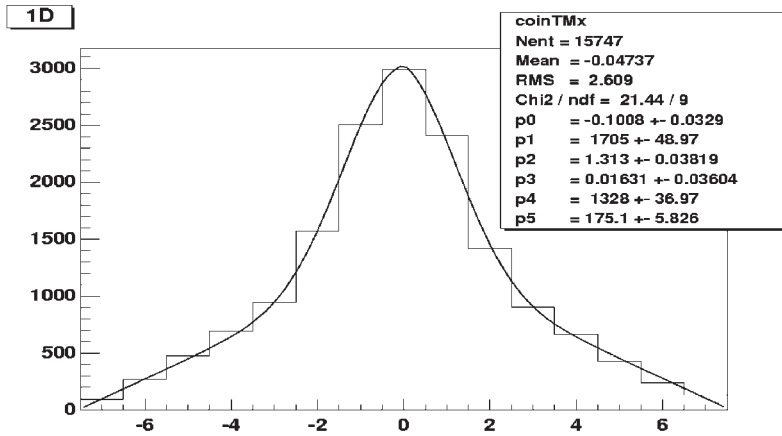


Fig. 33 Shift histogram with windows on BPMs

Now the central peak is more visible. From our past experience, we know that the triangular background is mainly due to the accidental coincidence between L and R counters. To estimate the triangular background, we moved one of the counters in the past so that the back-to-back double-gamma events are not recorded. Instead, this time, we applied a gate on the L-R time difference spectrum and took the events in the non-coincident region, namely channels 40 - 400 and 3500 - 4000. The "shift" spectrum thus obtained is shown in Fig. 34.

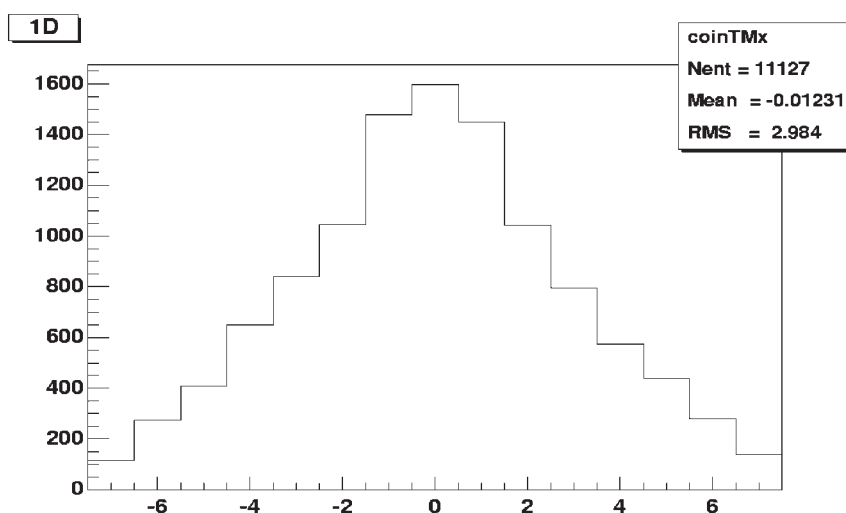


Fig. 34 Accidental coincidence spectrum of the shift

Now, we subtracted the spectrum shown in Fig. 34 multiplied an arbitrary factor from the spectrum shown in Fig. 33. The result is shown in Fig. 35.

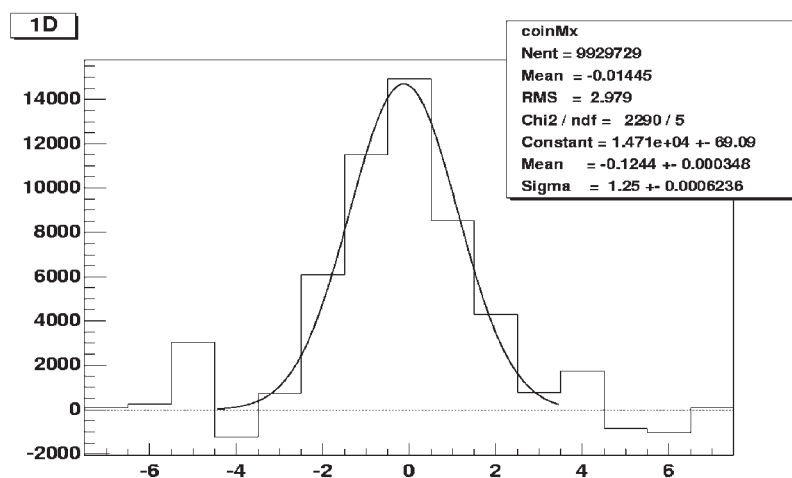


Fig. 35 Shift histogram obtained by subtracting the accidental coincidence events.

By fitting this histogram with a single Gaussian, the width of the peak was found to be 1.25 mm (RMS).

This value cannot be directly compared with the spatial resolution obtained with a measurement with a collimator (0.44 mm RMS), as the definition is different on one side, and on the other side, we have to remove the effect of the source spot size in the coincidence measurement.

Nevertheless, the shift of 1.25 mm should correspond to a spatial resolution of 0.6 mm (RMS) in terms of distinction of two source positions detected and reconstructed with two counters.

7. Summary

We tried a readout of LYSO crystal ($1\text{ mm} \times 1\text{ mm} \times 20\text{ mm}$) matrix using Y-11 wave-length shifter. In this readout, the natural background effect due to the radioactive isotope of ^{176}Lu is important, and all the measurement requires ^{22}Na source and coincidence measurements.

The self absorption effect of this crystal was experimentally measured using $1\text{ mm} \times 1\text{ mm} \times 40\text{ mm}$ crystal and a collimator. The result found was 12.9%/cm.

We added a back photomultiplier (BPM) to the old detector setup. This seems to collect about 50% photons leaked from the backside of the crystal pad after the WLS. The information obtained from BPM allows to distinguish between photopeak and the Compton process. It allowed us to make efficient cuts on the events to single out clean events, and at the same time to estimate the effect of background due to the backscattering of gamma.

Although there is some mismatch between the wave length of the emitted light of the WLS and the most sensitive wave length of the photocathode, LYSO - Y11 combination gives much more light in terms of the number of photoelectrons obtained at the PM. The use of 3M #9483 adhesive film improves considerably the light transmission to the WLS from the crystal. Also the light transmission to the PM is improved by the application of aluminized mylar sheet after the polishing of the open end of the WLS. The amount of photoelectrons so far obtained is 12.8.

We made a simulation of the light transmission inside the WLS. Comparison with the experiment reveals that the outside of the outer clad does not reflect totally the internal light. Thus the use of double-clad WLS is preferable.

We also made a simulation of the light generation and transmission inside the crystal using EGS software. Assuming 7% transmission of the light to the back side of the pad, 50% of light leakage to BPM reproduces a pulse-height distribution similar to the one obtained experimentally.

Spatial resolution was measured with a single crystal pad and NaI(Tl) counter in coincidence together with a ^{22}Na source. The resolution obtained was 0.44 mm. The peak/background ratio was initially 3.60. But by applying BPM pulse-height, and the time difference cuts, this ratio was improved to 25.4. The backscattering background seems small in this setup.

Spatial resolution was also measured with two LYSO detectors in coincidence. When the triangular background due to the accidental coincidence between the two counters is removed after applying different windows, the resolution expressed in terms of "shift" is 1.25 mm (RMS). The

backscattering background effect seems to be small in this setup.

Thus in conclusion, the progress is clear. We plan to make a measurement of the real spatial resolution similar as in a real PET in the near future.

Acknowledgement

The authors would like to thank Prof. M. Toyama for his constant encouragement and help.

This work has been supported by the Science Research Promotion Fund from the Promotion and Mutual Aid Corporation for private Schools of Japan, and a grant from Research Institute of Advanced Technology, Kyoto-Sangyo University.

References

- [1] F. Takeutchi and S. Aogaki, Read-out of a YAP array detector using wave-length shifter, Proc. Internat. mini - Workshop for Scintillating Crystals and their Applications Nov. 2003, KEK pp. 213-218,
F. Takeutchi, K. Okada and S. Aogaki, Test of non-perturbative QCD by means of the measurement of the K-pi scattering length,
Bulletin Inst. Comprehensive Res. Kyoto-Sangyo Univ. I (2003) pp. 15-38,
F. Takeutchi, et al., Test of non-perturbative QCD by means of the measurement
of the K-pi scattering length II, Bulletin Inst. Comprehensive Res. Kyoto-Sangyo Univ. II (2004) pp. 1-17
F. Takeutchi and S. Aogaki, Development of a high-resolution fast gamma-ray imager for the new-generation PET, Bulletin of the Research Institute of Advanced Technology, Kyoto Sangyo University, Vol. 4 (2005) pp. 45 - 67
- [2] F. Takeutchi and S. Aogaki, Read-out of scintillator crystal matrix using wave-length shifter, Proceedings of the Eighth International Conference on Inorganic Scintillator and their Use in Scientific and Industrial Applications, SCINT2005, pp 298-302
F. Takeutchi and S. Aogaki, Read-out of scintillator crystal matrix using wave-length shifter
- [3] <http://www.slac.stanford.edu/egs/>